Applied Catalysis B: Environmental 152–153 (2014) 241–249

Contents lists available at ScienceDirect

Applied Catalysis B: Environmental

journal homepage: www.elsevier.com/locate/apcatb

Alkylation of thiophenic compounds over heteropoly acid $H_3PW_{12}O_{40}$ supported on MgF_2

Frédéric Richard[a,*], Stéphane Célérier[a], Morgane Vilette[a], Jean-Dominique Comparot[a], Valérie Montouillout[b]

[a] Institut de Chimie des Milieux et Matériaux de Poitiers (IC2MP), UMR CNRS 7285, Faculté des Sciences Fondamentales et Appliquées, Université de Poitiers, 4, rue Michel Brunet, BP633, 86022 Poitiers Cedex, France
[b] CNRS, CEMHTI UPR 3079,Université d'Orléans 1D av. Recherche Scientifique, 45071 cedex 2 Orléans Cedex 2, France

ARTICLE INFO

Article history:
Received 19 November 2013
Received in revised form 10 January 2014
Accepted 15 January 2014
Available online 22 January 2014

Keywords:
Alkylation
Benzothiophene
Thiophene
Heteropoly acid
MgF_2

ABSTRACT

The alkylation of sulfur-containing compounds (benzothiophene and thiophene) with 2-methyl-1-pentene was investigated over MgF_2-supported heteropoly acid ($H_3PW_{12}O_{40}$: HPW) as catalysts under mild conditions (85 °C, atmospheric pressure). The magnesium fluoride used as support was prepared by a sol–gel method and exhibited a high specific surface area (186 $m^2\,g^{-1}$). Several solids containing various amounts of HPW (in the range of 5 wt% to 46 wt%) were prepared by incipient wetness impregnation and fully characterized (ICP–OES, XRD, N_2 adsorption, TEM, IR, adsorption of pyridine followed by IR, ^{19}F and ^{31}P MAS NMR).

For all solids, it was observed that the Keggin structure of HPW was preserved and that the heteropoly acid was finely dispersed on the MgF_2 support. A significant modification of the textural properties of the sample containing the higher amount of HPW (46 wt%) was observed and attributed to a pore blocking phenomenon by HPW. As expected, the HPW loading in the range of 5–30 wt% allowed an increase of the Brønsted acidity.

Whatever the catalyst, benzothiophene was only transformed by mono-alkylation, whereas the olefin underwent alkylation, oligomerization and isomerization, the latter being largely predominant and yielded 2-methyl-2-pentene. The increase of the HPW loading until 30 wt% led to an increase of the catalytic activity, the selectivity being not modified. In addition, a significant deactivation of catalysts containing 30 wt% and 40 wt% of HPW was observed and attributed to a strong adsorption of the alkylated products. Thiophene presented a poor reactivity through alkylation compared to benzothiophene.

1. Introduction

Owing to their strong Brønsted acidity, Keggin type heteropoly acids (HPA) exhibit a high activity in a wide variety of acid-catalyzed reactions [1,2]. The Keggin structure $XM_{12}O_{40}^{n-}$ consists of a central XO_4 tetrahedral group surrounded by 12 MO_6 octahedral groups as a shell, linked together by shared oxygen atoms [3]. The most typical Keggin heteropoly acids are $H_3PW_{12}O_{40}$, $H_4SiW_{12}O_{40}$, $H_3PMo_{12}O_{40}$ and $H_4SiMo_{12}O_{40}$, the former (hereafter HPW) being reported as the most acidic [1,2]. Due to a low specific surface area of bulk HPAs (close to 5 $m^2\,g^{-1}$), many attempts have been made to support heteropoly acid using various materials which can be acidic or neutral solids. Amorphous silica is by far the most commonly used in academic works [4–13] since it interacts weakly with the HPAs allowing to preserve their structure. Ordered mesoporous silica (MCM-41 [14–17] and SBA-15 [18–21]), ZrO_2 [22,23], and MgF_2 [24] are also chosen as support of HPW.

The solids based on supported 12-tungstophosphoric acid (HPW) were reported as effective catalysts for alkylation of aromatics [4,5,14,18,21,22] and thiophenic compounds [7,8]. A beneficial role of support for the alkylation of 4-*t*-butylphenol by isobutene was highlighted since HPW/MCM-41 exhibited higher catalytic activity than bulk HPW [14]. As an example, it was shown that the alkylation of phenol by *t*-butyl alcohol over HPW/SBA-15 with different loadings of HPW (10–70 wt%) led mainly to 4-*t*-butyl phenol, their activity depending on the HPW loading [19]. Indeed, the HPW/SBA-15 catalyst containing 30 wt% of HPW was the most active. In the same way, Sheng et al. reported that HPW supported on LaSBA15 containing the same loading of HPW (30 wt%) presented the best activity for the alkylation of *o*-xylene with styrene

* Corresponding author. Tel.: +33 549 453 519; fax: +33 549 453 899.
E-mail address: frederic.richard@univ-poitiers.fr (F. Richard).

0926-3373/$ – see front matter © 2014 Elsevier B.V. All rights reserved.
http://dx.doi.org/10.1016/j.apcatb.2014.01.029

[21]. The alkylation of benzene with 1-dodecene was studied over HPW/SiO_2 [4] and HPW/SBA-15 [18], the latter being more active than a HY zeolite.

The alkylation of thiophenic compounds is particularly interesting to reduce the sulfur content of gasoline feedstocks in the context of sulfur content reduction in gasoline marketed in European countries (less than 10 ppm since 2009) [25]. In this regard, the OATS (Olefinic Alkylation of Thiophenic Sulfur) process, firstly developed by British Petroleum [26], consists in an increase of the molecular weight of the sulfur containing compounds through alkylation with olefins present in the FCC cut naphtha over acid catalysts followed by a distillation. This process does not require hydrogen, the olefins responsible for good octane number are thus not hydrogenated, intended for conservation of a great quality of the desulfurized gasoline. Nevertheless, the side-reaction of olefin oligomerization has to be prevented in order to limit the consumption of light olefins. Thiophenic compounds are often chosen as probe sulfur-containing molecules since they are known to be the major sulfur impurities likely present in the FCC cut naphtha [27,28]. Acidic zeolites were often used as catalysts to study the alkylation of thiophenic compounds [29–33]. Silica-supported HPW was also reported as an efficient catalyst for the alkylation of 3-methylthiophene with 2-methyl-2-butene at 85 °C under atmospheric pressure [7,8].

Due to its inert surface, high thermal stability and hardness, magnesium fluoride (MgF_2) has been successfully used as support of metals or oxides in different catalytic processes [24,34–38]. For example, HPW supported on MgF_2 was found as an efficient catalyst for oligomerization of isobutene [24]. It was observed that the reaction rate depended on the HPW loading, a maximum of activity was observed for the catalyst containing about 30 wt% of HPW. Nevertheless, the specific surface area of MgF_2 support used in this study was relatively low (31 $m^2\,g^{-1}$). The use of MgF_2 support presenting higher specific surface areas is supposed to favor the dispersion of HPW and hence to increase the catalytic activity. In this way, Kemnitz and co-workers [39,40] had recently developed a new sol–gel synthesis of MgF_2 which exhibited very high specific surface areas (ranging from 200 to 500 $m^2\,g^{-1}$, depending on the synthesis parameters). These high specific surface areas modify the organization of the surface leading to a high density of acid sites with moderate strength. These materials had also a mesoporous structure and a nanoscopic particle dimension. This type of MgF_2 was successfully used as support of metals, oxides and perfluorosulfonic acid active species [38–41].

The aim of the present study was to evaluate the catalytic behavior of HPW supported on MgF_2 for the alkylation of sulfur-containing compounds (thiophene and benzothiophene) by an olefin (2-methyl-1-pentene) under mild conditions (85 °C, atmospheric pressure). For this purpose, HPW/MgF_2 samples containing 5–46 wt% HPW were prepared by impregnation of the synthesized MgF_2 obtained by a sol–gel method and were fully characterized by inductively coupled plasma–optical emission spectrometry (ICP–OES), nitrogen sorption, X-ray diffraction (XRD), Fourier transform infrared spectroscopy (FT-IR), transmission electron microscopy (TEM), ^{19}F and ^{31}P High Resolution Solid State NMR spectroscopy, adsorption of pyridine followed by infrared spectroscopy. Our objective was to correlate the structural, microstructural and physico-chemical properties of the MgF_2-supported HPW catalysts with their catalytic properties in alkylation of thiophenic compounds.

2. Experimental

2.1. Catalyst preparation

MgF_2 powder was prepared by a sol–gel method described by Wuttke et al. [42]. In a first step, magnesium metal (1.56 g, Aldrich, 99.98%) was treated with methanol excess (50 mL, Sigma-Aldrich, 99.8%) under reflux conditions for 6 h to form $Mg(OCH_3)_2$ metal alkoxide solution. Then, stoichiometric amount of aqueous HF (5.3504 g, 48 wt% in water, Sigma-Aldrich, 99.99%) was added to this solution under stirring conditions. A highly exothermic reaction was performed to form the sol (gel was not formed due to the stirring conditions). This sol was then stirred for 24 h, aged at ambient temperature for 24 h and dried at 100 °C for 24 h. The final MgF_2 support was obtained after calcination at 200 °C for 3 h in air in a flow-through tube furnace.

12-Tungstophosphoric acid hydrate $H_3PW_{12}O_{40}$, xH_2O (Sigma-Aldrich, reagent grade) was supported over MgF_2. Supported-MgF_2 HPW, referred to as *x*%HPW/MgF_2 (*x* = 5, 15, 30, 46), which *x*% corresponds to the theoretical weight content of HPW, were prepared by incipient wetness impregnation on as-prepared MgF_2 powder from methanolic solution of HPW. In a first step, HPW was dried at 200 °C in a furnace for 24 h to remove a part of water, $H_3PW_{12}O_{40}{\cdot}6H_2O$ (structure determined by XRD) was then obtained. Then, the desired amount of HPW (*x*%) was dissolved in methanol (1.6 mL) before deposition on 2 g of MgF_2. The as-prepared *x*%HPW/MgF_2 was aged at ambient temperature for 8 h and dried at 60 °C for one night before calcination at 200 °C for 3 h under air flow (4 L h^{-1}). The experimental values of HPW loading in *x*%HPW/MgF_2 obtained from ICP measurement were close to the theoretical amounts, as indicated in Table 1.

2.2. Catalyst characterization

The tungsten and magnesium contents of all catalysts were determined by inductively coupled plasma–optical emission spectrometry (ICP–OES) using a PerkinElmer Optima 2000DV instrument.

XRD analysis of material powders were carried out on a PANalytical EMPYREAN powder diffractometer using Cu *K*α radiation source ($K\alpha_1$ = 1.5406 Å and $K\alpha_2$ = 1.5444 Å) in order to reveal the

Table 1
Physico-chemical characterizations of HPW/MgF_2 type materials.

Catalyst	Content of HPW[a] (wt%)	S_{BET}[b] ($m^2\,g^{-1}$)	V_{tot}[c] ($cm^3\,g^{-1}$)	Estimated surface of HPW[d] ($m^2\,g^{-1}$)	Monolayer fraction of HPW[e] (%)
MgF_2	–	186	0.35	0	–
5%HPW/MgF_2	5.2	171 (180)[f]	0.32 (0.34)[f]	16	9
15%HPW/MgF_2	15.0	152 (179)[f]	0.26 (0.31)[f]	49	32
30%HPW/MgF_2	28.7	121 (170)[f]	0.20 (0.28)[f]	98	86
46%HPW/MgF_2	46.3	74 (137)[f]	0.09 (0.17)[f]	150	202

[a] Deduced from ICP analysis.
[b] Specific surface area calculated by the BET method.
[c] Total pore volume determined at P/P_0 = 0.99.
[d] Surface of HPW estimated by taking into account the weight of HPW and the area occupied per Keggin anion (156 $Å^2$) [46].
[e] Monolayer fraction calculated by the ratio between the estimated surface of HPW and the total surface measured by the BET method.
[f] In brackets are values after correction due to the contribution of the weight gain consecutive to the introduction of HPW.

crystallographic structure of each sample. These patterns were collected with a 0.07° step and 150 s dwell time at each step between 15° and 70°. Phase identification was performed by comparison with the JCPDS database reference files.

Nitrogen adsorption–desorption were recorded at −196 °C using a TRISTAR 3000 gas adsorption system. Prior N_2 adsorption, the powder samples were degassed under secondary vacuum for 1 h at 90 °C and 10 h at 180 °C. The specific surface area of each solid (S_{BET} in $m^2\,g^{-1}$) was calculated from the adsorption isotherms using the BET method [43]. The total pore volume (V_{tot}) was calculated from the adsorbed volume of nitrogen at P/P_0 equal to 0.99.

Infrared spectra of all samples were recorded on a FT-IR spectrometer (ThermoNicolet NEXUS 5700) in a wavenumber range of 4000–400 cm^{-1}. Absorbance measurements were carried out by making use of a KBr pellets containing 5 wt% of the powder sample to be analyzed.

The morphology of the MgF_2 support as well as the HPW particle size distribution for the 40%HPW/MgF_2 sample were evaluated by Transmission Electronic Microscopy (TEM), using a JEOL 2100 instrument (operated at 200 kV with a LaB_6 source and equipped with a Gatan Ultra scan camera).

All solid-state MAS NMR experiments were performed at room temperature on a Bruker Avance spectrometer operating at a magnetic field of 17.6 T (^{19}F and ^{31}P Larmor frequencies of 705.6 and 303.7 MHz, respectively) using a 2.5 mm double resonance MAS probehead and a spinning frequency of 33 kHz. To ensure quantitative analyses, the MAS spectra were acquired after a single pulse of 1 μs (corresponding to a flip angle of 45°) with a recycle delay of 10 s for ^{19}F, and of 2 μs (corresponding to a flip angle of 45°) with a recycle delay of 60 s for ^{31}P. ^{19}F and ^{31}P chemical shifts were referenced relative to $CFCl_3$ and H_3PO_4 85% solution, respectively. All spectra were fitted using the DMfit program [44].

The acidity of materials was measured by adsorption of pyridine followed by FT-IR spectroscopy using a ThermoNicolet NEXUS 5700 spectrometer with a resolution of 2 cm^{-1} and 128 scans per spectrum. Material samples were pressed into thin pellets (10–30 mg) with diameter of 16 mm under a pressure of 1–2 t cm^{-2} and activated in situ during one night under vacuum (10^{-5} Pa) at 170 °C. Pyridine was introduced in excess at 150 °C after the activation period. The solid sample was vacuum-packed to eliminate physisorbed pyridine and IR spectrum was recorded at 150 °C. The concentrations of the Brønsted and Lewis sites were determined from the integrated area bands of the PyH^+ (located at 1539 cm^{-1}) and PyL (1447 cm^{-1}) species using the values of the molar extinction coefficients of both bands (1.13 and 1.28 cm μmol^{-1}, respectively).

2.3. Catalytic tests

The transformation of two model feedstocks was performed in a fixed bed reactor at 85 °C under atmospheric pressure. Benzothiophene (BT, Aldrich, 98%) and thiophene (T, Aldrich, 98%) were used as model thiophenic compounds, 2-methyl-1-pentene (2M1P, Aldrich, 98%) was chosen as the model olefin which acted as alkylating agent. *n*-Heptane (Aldrich, 97%) and *n*-decane (Aldrich, 99%) were also added in the model mixture, the latter was used as an internal standard for quantitative GC analysis. The compositions of both model feeds used were BT or T (5.1 mol%), 2M1P (23.4 mol%), *n*-decane (2.1 mol%) and *n*-heptane (69.4 mol%). No transformation of reactants was observed without catalyst.

Before each experiment, the solid sample (particle sizes in the range of 200–400 μm) was pretreated in situ at 200 °C for 12 h under dry air flow (60 mL min^{-1}). After cooling at the reaction temperature (85 °C), the liquid reactant mixture was introduced in the reactor through a syringe pump (4.8 mL h^{-1}). Nitrogen was used as a carrier gas (60 mL h^{-1}). All experiments were performed in the presence of 200 mg of catalyst. The molar flow of thiophenic compounds (T or BT) was set at 1.8 mmol h^{-1} to obtain conversions of sulfur-containing reactants lower than 50%. The molar flow of 2M1P was also kept constant for all experiments at 8.0 mmol h^{-1}.

The liquid effluents were collected at −5 °C (using a Minichiller Huber cryostat) and analyzed for different times on stream (between 30 min and 3 h) on a Varian 430 chromatograph equipped with a CPSIL-5CB capillary column (length: 50 m; diameter: 0.25 mm; film thickness: 0.4 μm) and a flame ionization detector. An analysis using a second chromatograph (Varian 3400) equipped with a Plot Fused Silica capillary column and a flame ionization detector was performed on-line to detect the presence of possible non condensed compounds.

The products were identified both by using GC/MS analysis (Varian 3800 chromatograph coupled with a 1200 TQ mass spectrometer), and by adding aliquots of commercial compounds.

The activity of each catalyst was calculated according to the following equation (considering a first order reaction):

$$A = -\frac{F}{W_{cat}}\mathrm{Ln}(1-x)$$

where A is the activity (in mol h^{-1} g^{-1}), F the molar flow of the considered reactant (BT, T or 2M1P), W_{cat} the weight of the catalyst (0.200 g), and X the conversion of the considered reactant determined after 30 min on stream.

The turn over frequency value (TOF in h^{-1}) was deduced from the activity considering only the Brønsted acid sites as active species and was calculated by the following equation:TOF = $\frac{A}{C_B}$where A is the activity of the catalyst and C_B the concentration of Brønsted acid sites determined by adsorption/desorption of pyridine at 150 °C followed by IR spectroscopy.

2.4. Characterization of the catalysts after reaction

After reaction performed at 85 °C, the catalyst was kept in the reactor under nitrogen flow (30 mL min^{-1}) during 1 h in order to eliminate physisorbed compounds. The amounts of carbon and sulfur remaining on the catalyst were measured by total burning at 1020 °C under helium and oxygen using an elementary analyser (NA2100 analyser, CE instruments). In order to obtain more insight about the nature of organic compounds remaining onto the spent catalyst, it was analyzed by IR after treatment at 200 °C under vacuum.

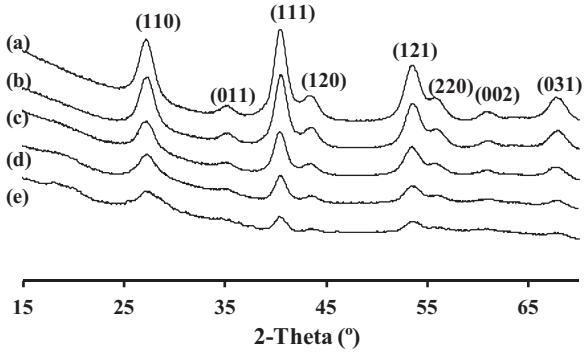

Fig. 1. X-ray diffraction patterns of *x*%HPW/MgF_2, with x = 0 ((a) bare MgF_2); 5 (b); 15 (c); 30 (d); 46 (e). The $h\,k\,l$ indices of the MgF_2 structure ($P42/mnm$ space group) are reported in brackets.

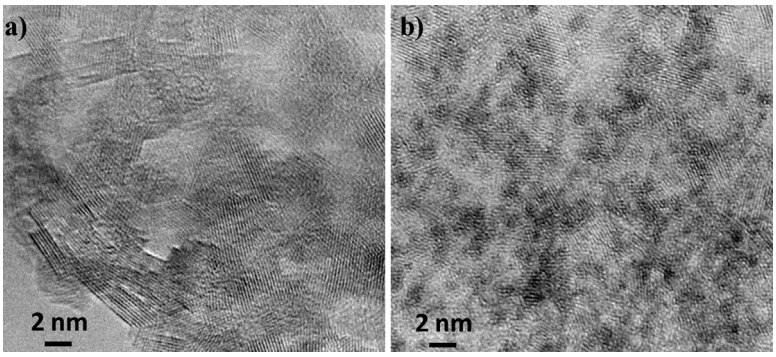

Fig. 2. TEM images obtained for MgF_2 (a) and 46%HPW/MgF_2 (b).

3. Results and discussion

3.1. Characterization of catalysts

The XRD diffraction patterns of bare MgF_2 and of the solids with different HPW loadings are shown in Fig. 1. All the solid samples exhibited the typical reflections of MgF_2, with main peaks at 27° (1 1 0) and 40° (1 1 1). It can be noticed that MgO was never observed by XRD in these samples, even for the bare MgF_2 heat-treated at 800 °C under air (not shown). This result is in agreement with those reported by Kemnitz and coworkers [39,42] using the same synthesis method. The crystallite size of MgF_2, calculated using the Debye–Sherrer equation applied to the (1 1 1) reflection at $2\theta = 40°$, was estimated at 6 nm for the bare MgF_2. This value is in good agreement with the TEM analysis of the host support showing well crystallized MgF_2 particles of size ranging from 4 to 6 nm (Fig. 2a). In addition, XRD diffraction patterns of all HPW/MgF_2 solids did not allow HPW reflection to be observed. This fact can be explained either by the formation of an amorphous phase of HPW, or by a HPW crystallization at a size below the detection limit (<3 nm) due to a high dispersion of HPW on MgF_2. In accordance with the last proposal, Fig. 2b shows that the 46%HPW/MgF_2 sample exhibited a good dispersion of the HPW particles (dark spheres) with very low size (below 2 nm) over the MgF_2 support.

Fig. 3 shows the adsorption–desorption isotherms of all solid samples. A type IV isotherm according to the IUPAC classification was observed whatever the HPW loading indicating the preservation of the organized network of the MgF_2 support in presence of HPW, which is in agreement with XRD results. The hysteresis presented a H_2 type which can be characteristic of the presence of ink bottle shaped pores [45]. The bare MgF_2 synthesized by a sol–gel method exhibited a high specific surface area (186 $m^2\,g^{-1}$) and a pore volume close to 0.68 $cm^3\,g^{-1}$ due to the interparticles voids (Table 1). The increase of the HPW loading from 5 to 46 wt% led to a decrease of both the specific BET specific surface area (S_{BET}) from 171 to 74 $m^2\,g^{-1}$ and of the total pore volume (V_{tot}) from 0.32 to 0.09 $cm^3\,g^{-1}$. Except for the 46%HPW/MgF_2 sample, this trend can be attributed to the weight gain consecutive to the introduction of the heteropolyacid. Indeed, the S_{BET} and V_{tot} values recalculated taking into account only the support weight remain constant with HPW loading between 5 and 30 wt%, as reported in Table 1. This indicates also that the surface generated by HPW is negligible. The important loss of both specific surface area and total porous volume observed for the 46%HPW/MgF_2 solid sample could be explained by a pore blocking of MgF_2 due to the high loading of HPW.

Taking into account the surface area occupied by a Keggin anion determined by Scanning Tunneling Microscopy images, which was found equal to 156 $Å^2$ [46], the theoretical surface area of a monolayer of HPW can be estimated according to Newman et al. [47]. The calculated values, given Table 1, showed that a fully dispersed HPW film would completely cover the MgF_2 support when the HPW loading was higher than 30 wt%.

It is well known that characteristic vibration bands due to the Keggin structure appeared in the region below 1200 cm^{-1} [48,49]. Fig. 4 shows the FT-IR spectra of bare MgF_2 and MgF_2 supported HPW samples in the range of 1200–700 cm^{-1}. According to literature [48,49], the band at 1082 cm^{-1} is assigned to ν_{as}(P–O), the broad band at 983 cm^{-1} to ν_{as}(W=O), the band at 896 cm^{-1} to ν_{as}(O–W–O) and the very broad band at 809 cm^{-1} to ν_{as}(W–O–W). As expected, the increase of the HPW loading led to an increase of the characteristic bands of HPW (Fig. 4). Consequently, the Keggin structure remained intact whatever the loading level of HPW over MgF_2.

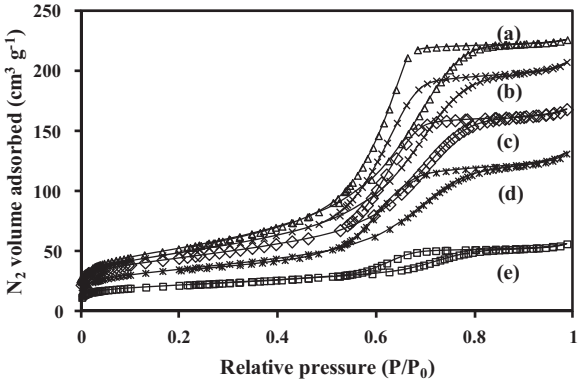

Fig. 3. Nitrogen adsorption–desorption isotherms of x%HPW/MgF_2 with $x = 0$ ((a) bare MgF_2); 5 (b); 15 (c); 30 (d); 46 (e).

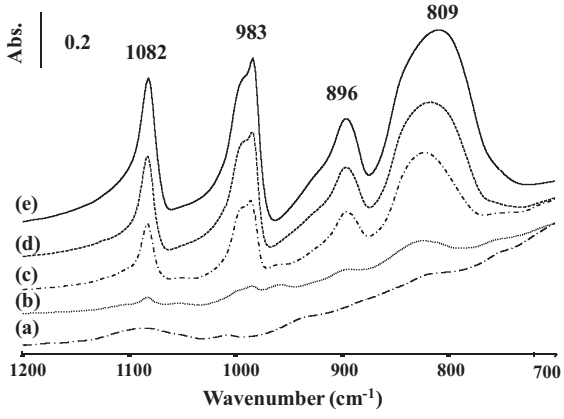

Fig. 4. FTIR spectra of x%HPW/MgF_2 with $x = 0$ ((a) bare MgF_2); 5 (b); 15 (c); 30 (d); 46 (e).

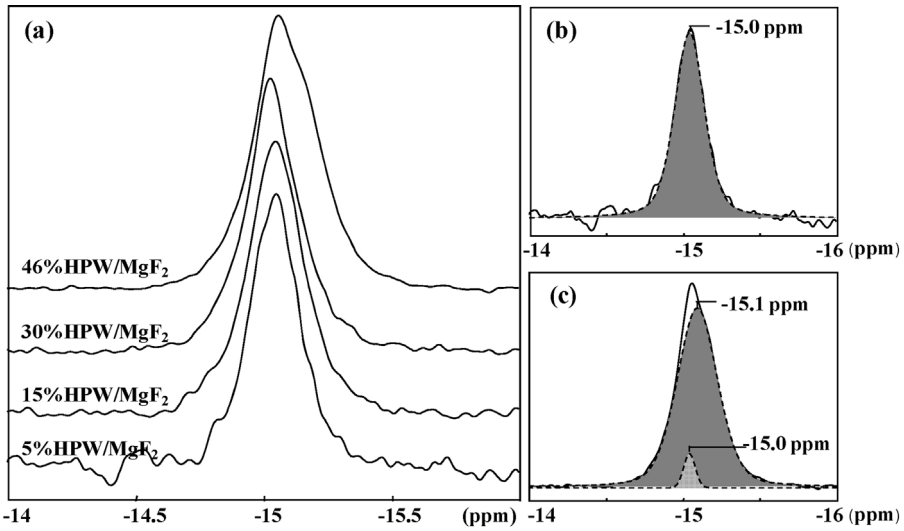

Fig. 5. ^{31}P MAS NMR spectra of *x*%HPW/MgF_2 with *x* equal to 5, 15 30 and 46 (a). Deconvolution of 5%HPW/MgF_2 (b) and 46%HPW/MgF_2 (c).

The ^{31}P MAS NMR spectra of the MgF_2-supported HPW are shown on Fig. 5. Up to a HPW loading of 30%, the spectra are composed of an unique signal centered at −15.0 ppm with a linewidth FWHM of 70 Hz (Fig. 5a) previously attributed to supported $H_3PW_{12}O_{40}$ [50,51]. At the highest HPW loading (46 wt%), the signal is slightly different and can be decomposed into two peaks, a sharp peak at −15.0 ppm (FHWM = 30 Hz) and the second broad peak at −15.1 ppm (FHWM = 100 Hz). Both of them correspond to supported $H_3PW_{12}O_{40}$, however the homogeneous broadening of the second signal, largely predominant (95%) is probably related to a lower mobility of HPW due to their closer vicinity.

Fig. 6 shows that ^{19}F MAS NMR spectra of all solids are similar, indicating that the structure of MgF_2 support is not modify by HPW addition, even at a high HPW loading, in line with XRD results. The main signal centered at −198.5 ppm corresponds to F^- ion surrounded by three Mg^{2+} ions as in the crystalline MgF_2 structure [39,41,52]. In addition, a small peak is observed at −184.6 ppm and could be assigned to MgF_5O or MgF_4O_2 units, as already proposed [39]. The presence of these species could be due to the presence of water during the sol–gel preparation that led to the formation of hydroxyl groups in the fluoride material [39].

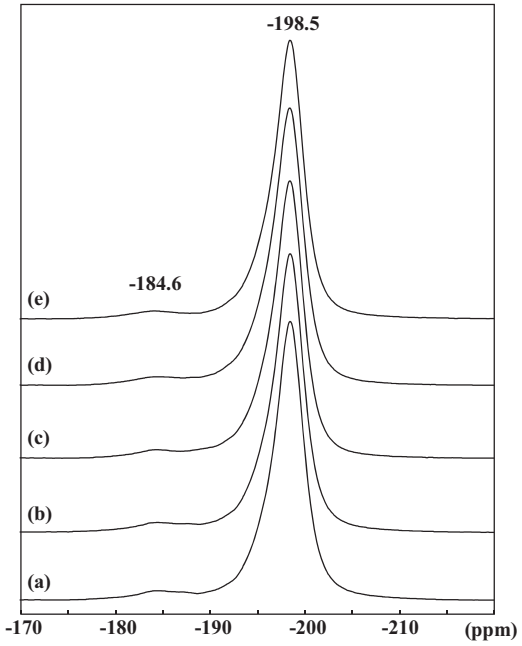

Fig. 6. ^{19}F MAS NMR spectra of bare MgF_2 (a) and *x*%HPW/MgF_2 with *x* equal to 5 (b); 15 (c); 30 (d); 46 (e).

The acidic properties of all samples were characterized by pyridine adsorption at 150 °C followed by IR analyses. The MgF_2 solid exhibited only Lewis acidity characterized by a band located at 1447 cm^{-1} (Table 2). This type of acidity can be attributed to the presence of five- and fourfold coordinate Mg^{2+} site on the surface, as already proposed by Agirrezabal-Telleria et al. [41]. As expected, the loading of HPW in the range of 5–30 wt% led to an increase of the Brønsted acidity, characterized by a band located at 1539 cm^{-1}, while the Lewis acidity remained roughly constant (Table 2). On the contrary, the Lewis acidity of 46%HPW/MgF_2 was reduced by half compared to the Lewis acidity of 30%HPW/MgF_2. This difference of acidity can be attributed to pore blocking of the support owing to the high HPW loading in the former, as proposed above based on the N_2 adsorption analysis, thus decreasing the number of accessible acid sites. This phenomenon, i.e. pore plugging by agglomeration of small HPW particles, can also explain why the Brønsted acidity was practically not modified when the HPW loading increased from 30 to 46 wt%. Indeed, a significant amount of HPW located inside the porous system of the 46%HPW/MgF_2 sample could be inaccessible to pyridine.

3.2. Transformation of the mixture BT-2M1P: Effect of the HPW loading

The transformation of BT in presence of 2M1P was carried out at 85 °C under atmospheric pressure over HPW/MgF_2 catalysts. It can be noticed that no product was observed from the BT-2M1P

Table 2
Acidic properties of catalysts determined by adsorption-desorption of pyridine followed by IR spectroscopy at 150 °C.

Catalyst	Brønsted acidity (μmol g^{-1})[a]	Lewis acidity (μmol g^{-1})[b]
MgF_2	3	260
5%HPW/MgF_2	16	269
15%HPW/MgF_2	58	291
30%HPW/MgF_2	154	265
46%HPW/MgF_2	157	135

[a] Deduced from the intensity of the band located at 1539 cm^{-1}.
[b] Deduced from the intensity of the band located at 1447 cm^{-1}.

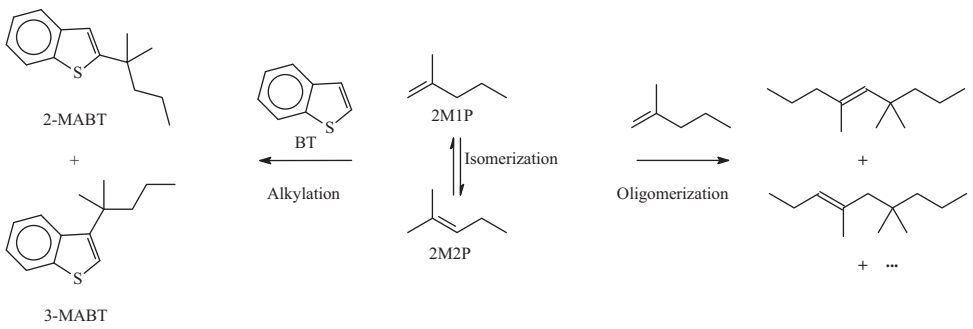

Scheme 1. Reactions involved during the transformation of the benzothiophene (BT)—2-methyl-1-pentene (2M1P) mixture over HPW/MgF_2 catalysts.

mixture when the bare MgF_2 sample was used as catalyst, showing that its Lewis acid sites were inactive.

Over HPW/MgF_2 catalysts, the reactions involved during the transformation of the BT-2M1P mixture are depicted in Scheme 1. BT underwent alkylation leading only to two monoalkylated products. The main isomer was alkylated on the α-position on the sulfur atom (2-MABT) and the minor on the β-position (3-MABT). Whatever the catalyst used, the 2-MABT/3-MABT ratio was higher than 3 (Table 3). Moreover, no alkylated products on the aromatic ring were detected showing that the aromatic ring of BT was not reactive by alkylation. Considering that the electrophilic alkylation of thiophenic compounds by olefins can proceed via a carbenium ion type mechanism [32], this product distribution can be explained by the difference of stability of the cationic intermediates. Indeed, using DFT calculations, it was shown that the cation leading to 2-MABT by deprotonation was much more stable than the carbenium ion leading to 3-MABT [33], in agreement with the fact that the position α to the sulfur atom is favored in the electrophilic substitution of thiophenes [53].

In addition to the alkylation products described above, 2M1P led to 2M2P (2-methyl-2-pentene) by double bond shift. This isomer was the main product obtained from 2M1P, its selectivity was close to 80 mol% over all catalysts (Table 3). Nevertheless, the presence of both isomers in the reaction mixture has no influence on the nature of the alkylated products since they lead to the same tertiary cation after their protonation, which is the alkylating agent. Two main olefins, containing 12 carbon atoms, were also detected but not identified. As an example, Scheme 1 presents the structure of two possible oligomers. These compounds were obtained from oligomerization of the 2M1P/2M2P mixture. This type of reaction has to be limited in order to reduce the consumption of light olefins into heavy ones. Fortunately, the alkylation products remained favored relative to the C_{12} olefins over all HPW/MgF_2 catalysts, their ratio being higher than 7 (Table 3).

Both the activity and the turn over frequency (TOF) values in BT alkylation and in 2M1P transformation are plotted as a function of the HPW loading (Figs. 7 and 8). In contrast to the selectivity of catalysts which was almost not influenced by the HPW loading, a significant effect of the content of HPW was highlighted on both activity and TOF values. Indeed, an increase of the activity was observed up to 30 wt%, while increasing the HPW loading at 46 wt% led to a low decrease of the activity in BT alkylation without modified the rate of the 2M1P isomerization (Fig. 7). This optimum activity in BT alkylation found for the 30%HPW/MgF_2 solid sample can be ascribed to its high Brønsted acidity, measured by pyridine adsorption (Table 2). In the case of 46%HPW/MgF_2, its lower activity in BT alkylation was probably due to the blocking of the acid sites owing to the presence of a multilayer Keggin structure, as discussed above, and allowing important diffusional constraints. This trend was also observed for various alkylation reactions catalyzed by HPW supported on SBA-15 [18,19,21]. Whatever the catalyst,

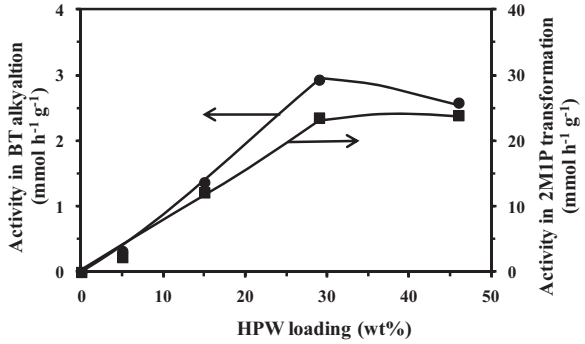

Fig. 7. Effect of the HPW loading on the activity for the benzothiophene (BT) alkylation (•) and for the 2-methyl-1-pentene (2M1P) transformation (■) at 85 °C under atmospheric pressure.

2M1P was about 10 times more reactive than BT. This result can be explained by the fact that 2M1P mainly reacted through isomerization, which is a less-demanding acid catalyzed reaction than alkylation.

The TOF values were calculated for each catalyst considering only Brønsted acid sites as active for the transformation of both reactants (BT and 2M1P) and plotted versus the HPW loading (Fig. 8). The 15%HPW/MgF_2 sample exhibited the higher value of TOF for BT alkylation and 2M1P transformation. At least two hypotheses may be suggested to explain the dependence of the TOF values with the HPW loading. On the one hand, a strong interaction between the heteropolyanion and the support can occur at a low HPW loading (less than 15 wt%) and leads to a decrease of the intrinsic activity of the Brønsted acid sites of the Keggin structure. This proposition is in accordance with the study reported by Mastikhin et al. [24] where supported MgF_2 with different loadings of

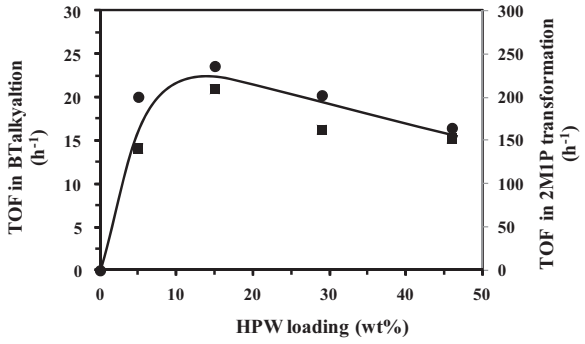

Fig. 8. Effect of the HPW loading on the Turn Over Frequency (TOF) for the benzothiophene (BT) alkylation (●) and for the 2-methyl-1-pentene (2M1P) transformation (■) at 85 °C under atmospheric pressure.

Table 3
Effect of the HPW loading on MgF_2 on the distribution of alkylated products from the transformation of the BT/2M1P mixture at 85 °C under atmospheric pressure.

Catalyst	Selectivity in sulfur-containing products (mol%)[a]		Selectivity in 2M1P products (mol%)[b]		
	2-MABT	3-MABT	2M2P	Alkylated products	C_{12} olefins
5%HPW/MgF_2	75.5	24.5	77.1	21.5	1.4
15%HPW/MgF_2	77.4	22.6	84.8	13.5	1.7
30%HPW/MgF_2	78.7	21.3	86.9	11.5	1.6
46%HPW/MgF_2	78.9	21.1	85.3	13.4	1.3

[a] Distribution of products determined at a conversion of BT close to 5%.
[b] Distribution of products determined for a conversion of 2M1P close to 20% (except for 5%HPW/MgF_2: the 2M1P conversion was close to 5%).

HPW were used as catalysts for the isobutylene oligomerization. On the other hand, the accessibility of reactants to acid sites is probably reduced at higher content of HPW (more than 30 wt%) due to the presence of a multilayer of Keggin structure, hence leading to a lower intrinsic activity of Brønsted acid sites in these cases. This may explain the lowest TOF values measured over both 30%HPW/MgF_2 and 46%HPW/MgF_2 compared to the one determined over 15%HPW/MgF_2.

Under the same operating conditions, acidic zeolites were found more active than HPW supported on MgF_2 for the BT alkylation by 2M1P [33]. For example, HMCM-22 was only 1.4 times more active than 30%HPW/MgF_2 whereas HY was 10 times more active. Nevertheless, as the alkylation to oligomerization ratio was equal to 7.6 for 30%HPW/MgF_2 and lower for HY (close to 5.7) [33], the former catalyst was more selective into BT alkylation compared to olefin oligomerization, the last reaction must be as limited as possible in order to reduce the olefin consumption during such process.

3.3. Study on the stability of HPW-based catalysts: Comparison between 30%HPW/MgF_2 and 46%HPW/MgF_2

The effect of time on stream on the conversion of both BT and 2M1P over 30%HPW/MgF_2 and 46%HPW/MgF_2 catalysts is depicted in Fig. 9. As discussed above, the initial conversion of BT was slightly higher over 30%HPW/MgF_2 (28%) than over 46%HPW/MgF_2 (25%). Concerning 2M1P, this olefin had the same initial reactivity over both catalysts: its conversion measured after 30 min on stream was close to 44% whatever the catalyst.

The deactivation rate of both catalysts can be estimated by the calculation of their residual activity, i.e. the ratio between the conversion measured after 180 min on stream and 30 min on stream. The deactivation rate depended on both the reactant (BT-2M1P) and the catalyst (30%HPW/MgF_2–46%HPW/MgF_2), as shown in Table 4. Concerning the influence of the reactant on the catalyst deactivation, it was observed that the residual activity was higher for the 2M1P transformation compared to the alkylation of BT in presence of both catalysts. These results show that isomerization, the main reaction involved during the transformation of 2M1P, is hence less sensitive to deactivation than alkylation. In addition, whatever the reactant, the 46%HPW/MgF_2 solid sample was deactivated faster than 30%HPW/MgF_2.

In order to better understand the deactivation process of the HPW/MgF_2 catalysts involved during the transformation of the BT-2M1P mixture at 85 °C, both spent catalysts were analyzed by chemical analysis and by FT-IR in order to identify and quantify the products remaining adsorbed onto the catalyst after reaction. The influence of these compounds on the textural properties of both catalysts was also investigated using N_2 adsorption.

Despite a low content of carbon (near 2.2 wt%) of the spent 46%HPW/MgF_2 catalyst, a significant loss of both specific surface area (−73%) and total pore volume (−67%) of this catalyst was observed (Table 4), which could explain the highest level of deactivation of this catalyst compared to 30%HPW/MgF_2 (Fig. 9). These results could be explained by the pore blocking resulting from the presence of the high HPW loading as discussed in the precedent section.

In addition, the *C*/*S* ratio of products remaining onto both spent catalysts was close to 4.6, which is similar to the one of a monoalkylated isomer (equal to 5.2). This seems to indicate that the compounds remaining adsorbed on both catalysts are mostly monoalkylated products. The IR spectra of the spent catalysts showed the same bands in the 3400–1300 cm^{-1} region (Fig. 10), which can be assigned to $\nu(CH)_{aromatic}$ (3084 cm^{-1}), $\nu(CH)_{aliphatic}$ (2964, 2929 and 2877 cm^{-1}), $\nu(CC)_{aromatic}$ (1699, 1590 and 1462 cm^{-1}) and $\delta(CH)_{aliphatic}$ (1420 cm^{-1}). Accordingly, the catalyst deactivation could also be attributed to a strong adsorption of alkylated products on the Brønsted acid sites of the MgF_2 supported heteropoly acid leading to a poisoning of such acid sites, as often proposed to explain the deactivation process of solid catalysts [54].

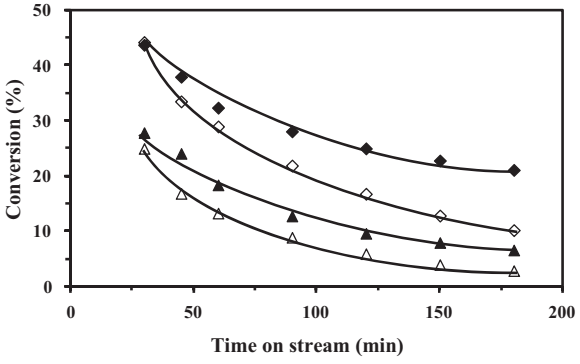

Fig. 9. Effect of time on stream on the conversion of BT (▲,△) and on the conversion of 2M1P (♦,◊) over 30%HPW/MgF_2 (full symbols) and 46%HPW/MgF_2 (empty symbols) at 85 °C under atmospheric pressure.

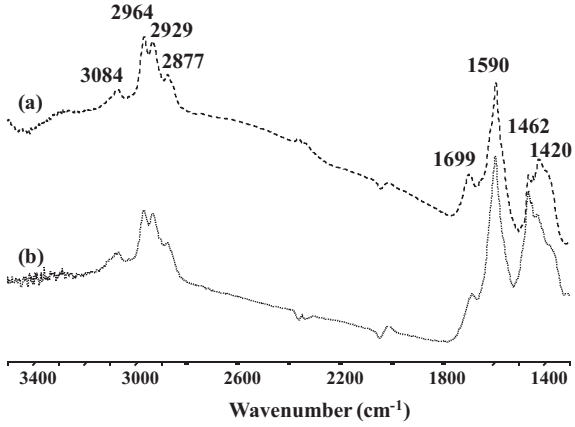

Fig. 10. Difference of IR spectra recorded after evacuation at 200 °C under vacuum for 30 min between spent and fresh catalysts. (a) 30%HPW/MgF_2; (b) 46%HPW/MgF_2.

Table 4
Residual activity and physico-chemical properties of the 30%HPW/MgF_2 and 46%HPW/MgF_2 spent catalysts after the alkylation of benzothiophene (BT) by 2-methyl-1-pentene (2M1P) at 85 °C under atmospheric pressure.

Catalyst	Residual activity (%)[a]		Chemical composition (wt%)		Textural properties[b]	
	BT	2M1P	*C*	*S*	S_{BET} ($m^2\ g^{-1}$)	V_{tot} ($cm^3\ g^{-1}$)
30%HPW/MgF_2	29	48	4.3	0.9	93 (23%)[c]	0.15 (25%)[c]
46%HPW/MgF_2	11	23	2.2	0.5	20 (73%)[c]	0.03 (67%)[c]

[a] Calculated by the ratio between the conversion of BT or 2M1P measured after 180 min and the conversion measured after 30 min.
[b] Determined by N_2 absorption.
[c] The values in brackets correspond to the loss (in percent) calculated from the values obtained for the fresh catalysts (reported in Table 1) and those measured over the spent catalysts.

Table 5
Effect of the thiophenic reactant on the activity and selectivity of 30%HPW/MgF_2 during the transformation of thiophene (T) or benzothiophene (BT) in presence of 2-methyl-1-pentene (2M1P) at 85 °C under atmospheric pressure.

	Activity ($mmol\ h^{-1}\ g^{-1}$)		Selectivity in sulfur-containing products (mol%)[a]		Selectivity in 2M1P products (mol%)[b]		
	Thiophenic compound	2M1P	Monoalkylated	Dialkylated	2M2P	Alkylated products	C_{12} olefins
T	0.2	37.3	26.1	73.9	96.9	1.3	1.8
BT	2.9	23.5	100.0	0.0	77.6	19.8	2.6

[a] Distribution of products determined at conversion less than 6%.
[b] Distribution of products determined for a conversion of 2M1P close to 38%.

3.4. Effect of the sulfur-containing product on the activity and selectivity of 30%HPW/MgF_2

Under the experimental conditions (85 °C under atmospheric pressure), *T* was found about 14 times less reactive than BT in alkylation over 30%HPW/MgF_2 (Table 5). This result could be due to a better stabilization of the cationic intermediates involved from the alkylation of BT because of the existence of the benzenic ring. It can also be noticed that 2M1P was more reactive in presence of T than in presence of BT, 2M2P, obtained by double bond shift, being in both cases the main reaction product of 2M1P. This result is in agreement with the fact that alkylated products, formed in larger quantities from BT compared to T, were strongly adsorbed on acid sites and hence partially inhibited isomerization of 2M1P into 2M2P.

The alkylation of T by 2M1P yielded two monoalkylated products and two dialkylated products. As observed when BT was used as reactant, the main monoalkylated isomer of T was alkylated on the α-position to the sulfur atom. This selectivity is also consistent with the higher reactivity of this position of the thiophenic ring than the β-position on the sulfur atom in the case of electrophilic addition [53]. As indicated in Table 5, the dialkylated compounds appeared as the main products of T even at a very low conversion of T (close to 3%), due to the activation effect of alkyl group for electrophilic addition, as proposed in [55]. On the opposite, the alkylation of BT led selectively to monoalkylated products, showing that (i) the formation of products containing two alkyl groups on the thiophenic ring is disfavored due to a significant steric hindrance, (ii) the aromatic ring of BT is not reactive in alkylation.

4. Conclusions

This study showed that the MgF_2 supported Keggin-type heteropoly acid ($H_3PW_{12}O_{40}$, HPW) solids were efficient catalysts for the alkylation of benzothiophene (BT) by 2-methyl-1-pentene (2M1P) under mild conditions (85 °C, atmospheric pressure). It was demonstrated that the use of MgF_2, synthesized by a sol–gel method leading to a high specific surface area, allowed a very good dispersion of the acid phase, the Keggin structure of HPW being maintained intact whatever its loading, ranging from 5 to 46 wt%.

A significant effect of the HPW loadings was highlighted on the activity of these catalysts, the 30%HPW/MgF_2 catalyst being the most active. For a higher loading (46 wt% of HPW), a decrease of both the specific surface area and the pore volume was attributed to pore blocking due to the presence of a multilayer HPW phase in this solid sample, thus contributing to its lower activity and its faster deactivation rate compared to the 30%HPW/MgF_2 catalyst.

Over all catalysts, BT underwent alkylation and led only to monoalkylated products, dialkylation was disfavored due to steric hindrance on the thiophenic ring. In addition to alkylation, 2M1P mainly reacted by isomerization, yielding 2-methyl-2-pentene, and by oligomerization. Fortunately, the latter reaction was always disfavored in a large extend compared to alkylation.

Moreover, the significant deactivation of these MgF_2 supported HPW catalysts which occurred during the transformation of the BT-2M1P mixture was mainly attributed to a strong adsorption of the alkylated products onto the Brønsted acid sites of the HPW phase.

The nature of the sulfur-containing reactant had also a notable influence on the activity of these catalysts. Indeed, thiophene (T) was found very less reactive than BT through alkylation, which was attributed to a low stability of the cationic intermediates involved during the alkylation of T.

Acknowledgment

Financial support from the TGIR-RMN-THC Fr3050 CNRS for conducting the research is gratefully acknowledged.

References

[1] I.V. Kozhevnikov, Chem. Rev. 98 (1998) 171–198.
[2] M.N. Timofeeva, Appl. Catal., A 256 (2003) 19–35.
[3] J.F. Keggin, Proc. R. Soc. London, Ser. A 144 (1934) 75–100.
[4] J. Zhang, Z. Zhu, C. Li, L. Wen, E. Min, J. Mol. Catal. A: Chem. 198 (2003) 359–367.
[5] Y. Kamiya, Y. Ooka, C. Obara, R. Ohnishi, T. Fujita, Y. Kurata, K. Tsuji, T. Nakajyo, T. Okuhara, J. Mol. Catal. A: Chem. 262 (2007) 77–85.
[6] V. Brahmkhatri, A. Patel, Kinet. Catal. 51 (2010) 380–384.
[7] M. Arias, D. Laurenti, C. Geantet, M. Vrinat, I. Hideyuki, Y. Yoshimura, Catal. Today 130 (2008) 190–194.
[8] M. Arias, D. Laurenti, V. Bellière, C. Geantet, M. Vrinat, Y. Yoshimura, Appl. Catal., A 348 (2008) 142–147.
[9] K.A. da Silva Rocha, N.V.S. Rodrigues, I.V. Kozhevnikov, E.V. Gusevskaya, Appl. Catal., A 374 (2010) 87–94.
[10] V.V. Costa, K.A. da Silva Rocha, I.V. Kozhevnikov, E.V. Gusevskaya, Appl. Catal., A 383 (2010) 217–220.
[11] E. Rafiee, M. Khodayari, S. Shahebrahimi, M. Joshaghani, J. Mol. Catal. A: Chem. 351 (2011) 204–209.
[12] A.L.P. de Meireles, K.A. da Silva Rocha, I.V. Kozhevnikov, E.V. Gusevskaya, Appl. Catal., A 409–410 (2011) 82–86.

[13] A.D. Newman, D.R. Brown, P. Siril, A.F. Lee, K. Wilson, Phys. Chem. Chem. Phys. 8 (2006) 2893–2902.
[14] I.V. Kozhevnikov, A. Sinnema, R.J.J. Jansen, K. Pamin, H. van Bekkum, Catal. Lett. 30 (1995) 241–252.
[15] I.V. Kozhevnikov, K.R. Kloetstra, A. Sinnema, H.W. Zandbergen, H. van Bekkum, J. Mol. Catal. A: Chem. 114 (1996) 287–289.
[16] L. Pizzio, G. Romanelli, P. Vasquez, J. Autino, M. Blanco, C. Caceres, Appl. Catal., A 308 (2006) 153–160.
[17] G. Karthikeyan, A. Pandurangan, J. Mol. Catal. A: Chem. 311 (2009) 36–45.
[18] J. Wang, H. Zhu, Catal. Lett. 93 (2004) 209–212.
[19] G. Satish Kumar, M. Vishnuvarthan, M. Palanichamy, V. Murugesan, J. Mol. Catal. A: Chem. 260 (2006) 49–55.
[20] X. Sheng, Y. Zhou, Y. Zhang, Y. Duan, Z. Zhang, Y. Yang, Microporous Mesoporous Mater. 161 (2012) 25–32.
[21] X. Sheng, Y. Zhou, Y. Zhang, M. Xue, Y. Duan, Chem. Eng. J. 179 (2012) 295–301.
[22] B.M. Devassy, G.V. Shanbhag, F. Lefebvre, S.B. Halligudi, J. Mol. Catal. A: Chem. 210 (2004) 125–130.
[23] B.M. Devassy, F. Lefebvre, S.B. Halligudi, J. Catal. 231 (2005) 1–10.
[24] V.M. Mastikhin, V.V. Terkih, M.N. Timofeeva, O.P. Krivoruchko, J. Mol. Catal. A: Chem. 95 (1995) 135–140.
[25] Off. J. Eur. Commun. L76 (2003) 10–19.
[26] B.D. Alexander, G.A. Huff, V.R. Pradhan, W.J. Reagan, R.H. Clayton, US Patent 6,024,865 (2000).
[27] C. Song, Catal. Today 86 (2003) 211–263.
[28] P. Ghost, A.T. Andrews, R.J. Quann, T.R. Halbert, Energy Fuels 23 (2009) 5743–5750.
[29] V. Belliere, C. Geantet, M. Vrinat, Y. Ben-Taârit, Y. Yoshimura, Energy Fuels 18 (2004) 1806–1810.
[30] V. Belliere, C. Lorentz, C. Geantet, Y. Yoshimura, D. Laurenti, M. Vrinat, Appl. Catal., B 64 (2006) 254–261.
[31] Z. Zhang, S. Liu, X. Zhu, Q. Wang, L. Xu, Fuel Process. Technol. 89 (2008) 103–110.
[32] B. Dupuy, S. Laforge, C. Morais, C. Bachmann, P. Magnoux, F. Richard, Appl. Catal., A 413–414 (2012) 192–204.
[33] B. Dupuy, S. Laforge, C. Bachmann, P. Magnoux, F. Richard, J. Mol. Catal. A: Chem. 363–364 (2012) 273–282.
[34] M. Wojciechowska, M. Zielinski, M. Pietrowski, J. Fluorine Chem. 120 (2003) 1–11.
[35] M. Pietrowski, M. Zielinski, M. Wojciechowska, ChemCatChem 3 (2011) 835–838.
[36] M. Zielinski, M. Pietrowski, M. Wojciechowska, ChemCatChem 3 (2011) 1653–1660.
[37] P.T. Patil, A. Dimitrov, H. Kirmse, W. Neumann, E. Kemnitz, Appl. Catal., B 78 (2008) 80–91.
[38] S.B. Troncea, S. Wuttke, E. Kemnitz, S.M. Cornan, V.I. Parvulescu, Appl. Catal., B 107 (2011) 260–267.
[39] S. Wuttke, S.M. Coman, G. Scholz, H. Kirmse, A. Vimont, M. Daturi, S.L.M. Schroeder, E. Kemnitz, Chem. Eur. J. 14 (2008) 11488–11499.
[40] S. Kemnitz, S.M. Wuttke, Coman, Eur. J. Inorg. Chem. (2011) 4773–4794.
[41] I. Agirrezabal-Telleria, F. Hemmann, C. Jager, P.L. Arias, E. Kemnitz, J. Catal. 305 (2013) 81–91.
[42] S. Wuttke, A. Vimont, J.-C. Lavalley, M. Daturi, E. Kemnitz, J. Phys. Chem. 114 (2010) 5113–5120.
[43] S. Brunauer, P.H. Emmett, E. Teller, J. Am. Chem. Soc. 60 (1938) 309–319.
[44] D. Massiot, F. Fayon, M. Capron, I. King, S. Le Calvé, B. Alonso, J.-O. Durand, B. Bujoli, Z. Gan, G. Hoatson, Magn. Reson. Chem. 40 (2002) 70–76.
[45] G. Leofanti, M. Padovan, G. Tozzola, B. Venturelli, Catal. Today 41 (1998) 207–219.
[46] M.S. Kaba, I.K. Song, D.C. Duncan, C.L. Hill, M.A. Barteau, Inorg. Chem. 37 (1998) 398–406.
[47] A.D. Newman, A.F. Lee, K. Wilson, N.A. Young, Catal. Lett. 102 (2005) 45–50.
[48] C. Hu, M. Hashimoto, T. Okuhara, M. Misono, J. Catal. 143 (1993) 437–448.
[49] N. Essayem, A. Holmqvist, P.Y. Gayraud, J.C. Vedrine, Y. Ben Taarit, J. Catal. 197 (2001) 273–280.
[50] M. Misono, Chem. Commun. 13 (2011) 1141–1152.
[51] F. Lefebvre, J. Chem. Soc., Chem. Commun. (1992) 756–757.
[52] M. Karg, G. Scholz, R. König, E. Kemnitz, Dalton Trans. 41 (2012) 2360–2370.
[53] A. Streitwieser Jr., C.H. Heathcock, Introduction to Organic Chemistry, Macmillian Publishing Co., Inc., New York, NY, 1976, pp. 1080–1082.
[54] P. Forzatti, L. Lietti, Catal. Today 52 (1999) 165–181.
[55] J. March, Advanced Organic Chemistry, third ed., John Wiley and Sons, Inc., New York, NY, 1985.